

Comparison of Markov Chain Monte Carlo and Generalized Least Square Methods on a Model of Glucose / Insulin Dynamics with GLP1-DPP4 Interaction

Sutharot Lueabunchong, Yongwimon Lenbury, Simona Panunzi, and Alice Matone

Abstract—In this paper, the performances of Markov Chain Monte Carlo (MCMC) method and Generalized Least Square (GLS) method are compared when they are used to estimate the parameters in a nonlinear differential model of glucose/insulin metabolism with GLP1-DPP4 interaction. The model is used to generate the data that consists of the time-concentration measurements of plasma glucose and of insulin, which are important in Diabetes Mellitus (DM) treatment. We show the results from three different runs to obtain parameter estimations by both MCMC and GLS. The true values (TV), point estimates (PM), standard deviation (SD) and 95% credible intervals (CI) of population parameters based on the two methods are presented. Our results suggest that MCMC is better able to estimate the parameters based upon smaller bias and standard deviation. Although MCMC requires more calculation time than GLS, it offers a more appropriate method, in our opinion, for nonlinear model parameter estimations without knowledge of the distribution of the data and when heterogeneity of variance is evident.

Keywords—glucose/insulin metabolism, GLS, MCMC, nonlinear differential equations model.

I. INTRODUCTION

DIABETES mellitus (DM) is a wide spread disease affecting an increasing number of people globally. It has

Manuscript received May 17, 2012; Revised version received May 17, 2012. This work was supported in part by the Strategic Scholarships Fellowships Frontier Research Network, the Office of Commission on Higher Education and, together with the third author, BioMatLab CNR-IASI, Italy. The second author is supported by the Centre of Excellence in Mathematics, CHE, Thailand.

S. Lueabunchong is with the Department of Mathematics, Faculty of Science, Mahidol University, Rama 6 Road, Bangkok 10400 and the Centre of Excellence in Mathematics, CHE, 328 Si Ayutthaya Road, Bangkok, THAILAND (e-mail: sutharot_luea@hotmail.com).

Y. Lenbury is with the Department of Mathematics, Faculty of Science, Mahidol University, Rama 6 Road, Bangkok and the Centre of Excellence in Mathematics, CHE, 328 Si Ayutthaya Road, Bangkok, Thailand (corresponding author, phone: 662-201-5448; fax: 662-201-5343; e-mail: yongwimon.len@mahidol.ac.th).

S. Panunzi is with the BioMatLab CNR-IASI, Fisiopatologia dello Shock University Cattolica del SacroCuore Largo A. Gemelli 8 - 00168 Roma, Italy (e-mail: simona.panunzi@biomatematica.it).

A. Matone is with the BioMatLab CNR-IASI, Fisiopatologia dello Shock University Cattolica del SacroCuore Largo A. Gemelli 8 - 00168 Roma, Italy (e-mail: alice.matone@libero.it).

in the past been a serious health concern for the developed countries, but is now discovered to effect more and more the less developed populations.

There are three major forms of diabetes: type 1 diabetes mellitus (T1DM, also known as insulin-dependent or juvenile-onset diabetes), type 2 diabetes mellitus (T2DM, also known as non-insulin-dependent or maturity-onset diabetes), and gestational diabetes.

The study of glucose and insulin metabolism is fundamental to the understanding of the mechanisms and the diagnosis of DM. Insulin is recognized as the central hormone that maintains glucose absorption by various cells, particularly from blood into muscular and adipose cells. Therefore, lack of insulin or the insensitivity of its receptors plays a central role in all forms of DM [1]. Gestational diabetes develops in a small percentage of pregnant women and usually resolves after parturition. T1DM affects less than 10% of diabetic people and is an autoimmune disease in which the destruction of pancreatic beta-cells causes insulin deficiency. T2DM is, instead, a progressive disease, typically associated with obesity. There are several mechanisms that can be involved in T2DM, such as defects in insulin receptors which lead to a compromised insulin sensitivity in peripheral tissues (peripheral insulin resistance) or in the liver (central insulin resistance). In peripheral insulin resistance, tissues do not absorb glucose properly, while in central insulin resistance, hepatic glucose output is not correctly inhibited leading to unnecessary glucose production. T2DM can also exhibit insulin secretion insufficiency when the pancreatic beta-cells are compromised.

All these scenarios lead to an excess of glucose in the blood, a condition called hyperglycemia, that can lead to a number of dangerous consequences. Loss of electrolytes, dehydration, and polydipsia are caused by frequent urination, known as polyuria. Calorie loss influences polyphagia, negative nitrogen balance, acidosis, and increased depth of breathing [1]. These and other hyperglycemia related problems can eventually cause coma and death [1].

In order to study insulin and glucose metabolism, several mathematical models [2, 3, 4, 5, 6, 7] have been proposed, describing the effect of DM in the attempt to answer questions related to physiological complications.

In the present study, we concentrate on the roles of Glucagon-like peptide-1 (GLP-1) and dipeptidyl-peptidase-4 (DPP-4) on the glucose/insulin metabolism. GLP-1 is secreted from the L-cells of the intestinal mucosa (mostly of the ileum) after meal ingestion and reduces post-prandial glycaemia, enhancing insulin secretion and delaying gastric emptying [8]. The enzyme DPP-4 is a peptidase that inactivates GLP-1 and rapidly reduces its circulating levels [9].

Here, we apply and compare two statistical methodologies for parameter estimation. The Markov Chain Monte Carlo method (MCMC), which is used in a Bayesian setting, implemented in the repeated measurement data framework, and the Generalized Least Square method (GLS), which is used in the classical statistical formulation, are used to estimate some parameters in a glucose/insulin model with GLP1-DPP4 interaction.

In this study, data on a fixed number of subjects are generated with errors from the glucose/insulin model with GLP1-DPP4 interaction, when the model and its numerical integration are implemented in MATLAB. We focus on the comparison between the two procedures performed in terms of the point and interval parameter estimators. We apply the Bayesian models for the hierarchical nonlinear framework, which is regarded as an extension of the nonlinear regression models to handle data from several individuals, to provide the intra- and inter-individual variation. Finally, the results are compared and analyzed.

II. PROCEDURE

A. Glucose/insulin model with GLP1-DPP4 interaction

We here introduce a model representing glucose and insulin homeostasis and accounting for the effects of GLP-1 and DPP-4 peptides. The model is used to generate data of individual glucose and insulin concentrations in time.

Glucose dynamics is described by three state variables, each one representing glucose in a different stage during its metabolism, from entering the body within the meal, to its final absorption into the blood stream. Glucose first appears in the stomach within the meal, it is then transferred to the gut (here the duodenum is considered), where it stimulates incretin (GLP-1) secretion, and finally is absorbed from the blood stream, where it exerts its action in stimulating insulin outflow from pancreatic beta-cells. Insulin, in turns, induces glucose absorption from peripheral tissues and inhibits hepatic glucose production, thus returning, in a healthy individual, plasmatic glucose concentration to basal levels. Insulin secretion from the pancreas is increased (this is why the term “incretin” is used) from GLP-1, which is released from the gut when glucose passes through it. GLP-1 is rapidly degraded from DPP-4, which is an ubiquitous enzyme, present in several forms and carrying out different actions in the body, depending on its location and specificity. The degradation of GLP-1 from DPP-4 is a safety mechanism which guarantees that, when glucose is not in the gut and its plasma concentration is not going to increase, incretins stop stimulating insulin secretion. Figure 1 gives a schematic description of the glucose/insulin

interaction with GLP1-DPP4 interaction. The referenced mathematical model of this process is as follows.

$$\frac{dS(t)}{dt} = -K_{ds}S(t), \quad S(t_0) = S_b \quad (1)$$

$$\frac{dD(t)}{dt} = K_{ds}S(t) - K_{gd}D(t), \quad D(t_0) = 0 \quad (2)$$

$$\frac{dG(t)}{dt} = -K_{xg}G(t) - K_{xgl}I(t)G(t) + \frac{K_{gd}D(t)}{V_g} + T_{gl}, \quad G(t_0) = G_b \quad (3)$$

$$\frac{dI(t)}{dt} = -K_{xi}I(t) + T_{iG}G(t) + T_{iGN}N(t)G(t), \quad I(t_0) = I_b \quad (4)$$

$$\frac{dN(t)}{dt} = T_{nD}D(t) - K_{xnp}P(t)N(t) - K_{xn}N(t) + T_n, \quad N(t_0) = N_b \quad (5)$$

$$\frac{dP(t)}{dt} = -K_{xp}P(t) + T_p, \quad P(t_0) = P_b \quad (6)$$

where S, D, G, I, N and P are, respectively: the amount of ingested glucose appearing in the stomach; glucose concentration in the duodenum; plasma glucose concentration; plasma insulin concentration; plasma GLP-1 concentration; plasma DPP4 concentration. In equation (1), the initial condition, S_b , represents the amount of ingested glucose, and the only term on the right hand-side represents glucose elimination from the stomach, where K_{ds} is the transfer rate from the stomach to the duodenum. Equation (2) describes the dynamics of glucose concentration in the duodenum. The first term represents the entry from the stomach, while the elimination term is plasma absorption, K_{gd} being the transfer rate constant from the duodenum to the blood. Equation (3) represents plasma glucose concentration dynamics. This is described by: insulin-independent glucose tissue uptake, where K_{xg} is the glucose-dependent elimination rate constant; insulin-dependent glucose tissue uptake, where K_{xgl} is the second order elimination rate constant, insulin and glucose-dependent; entry from the duodenum, where V_g in the denominator is the distribution volume for glucose; and the constant entry depending on liver release, where T_{gl} is the constant rate of hepatic glucose production.

Insulin dynamics is described by equation (4), the first term represents physiological insulin elimination, where K_{xi} is the disappearance rate constant. The two entries depend, respectively: on glucose concentration, T_{iG} being the production rate constant of pancreatic release of insulin due to glucose, and on GLP-1 stimulatory effect, where T_{iGN} is the rate of pancreatic release of insulin due to incretin action.

Equation (5) represents GLP-1 dynamics, where the first term corresponds to the release due to glucose concentration in the duodenum, T_{nD} being the D dependent constant production rate. GLP-1 elimination due to DPP-4 cleavage is represented by the second right term, where K_{xnp} is the

disappearance rate constant, GLP-1 and DPP-4 dependent. The physiological GLP-1 elimination is described by the third term where K_{xn} is the disappearance rate constant. A constant entry is also assumed, represented by the last term, where T_n is the constant production rate.

The last equation (6) describes DPP-4 dynamics, where K_{xp} in the elimination term is the disappearance rate, DPP-4 dependent, and the last term corresponds to DPP-4 production, where T_p is the appearance rate constant.

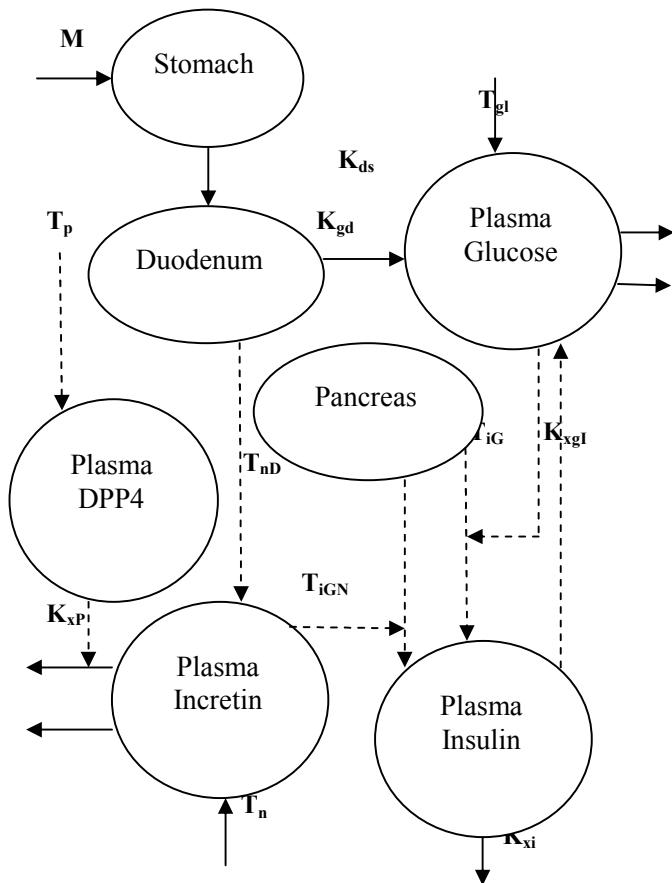


Fig.1 Schematic description of the glucose/insulin interaction with GLP1-DPP4 interaction.

B. Materials and Methods

The objective of this work is to estimate the unknown parameters K_{gd} , K_{xg} , K_{xgl} , K_{xi} and V_g in (3) and (4), describing the differences over time of concentration measurements of plasma glucose $G(t)$, and of insulin $I(t)$, by using MCMC and GLS methods. By using MATLAB, data and errors for 30 subjects were generated from the glucose/insulin nonlinear differential equations model with GLP1-DPP4 interaction. The data consist of the time concentration measurements of plasma glucose $G(t)$, and of insulin $I(t)$, every 10 minutes, ranging from 0 to 300 minutes,

during which $G_k(t)$ and $I_k(t)$ of the subject k were found. Table 1 reports the definition of all the quantities in (3) and (4).

Let us consider $y_{\chi kj} = f_{\chi kj}(\beta_k, t_{kj}) + e_{kj}$, where y_{kj} denotes the variable concentration of the subject $k; k=1,2,3,\dots,30$, at time $j; j=1,2,3,\dots,30$, while χ is equal to G for glucose or I for insulin. Then, $f_{\chi kj}(\beta_k, t_{kj})$ represents the prediction functions at time j for the k -th subject, which is derived from the numeric solution $\tilde{f}(\beta_k, t)$ of the following differential equation model:

$$\frac{dG(t)}{dt} = -K_{xg}G(t) - K_{xgl}I(t)G(t) + \frac{K_{gd}D(t)}{V_g} + T_{gl}, G(t_0) = G_b \quad (7)$$

$$\frac{dI(t)}{dt} = -K_{xi}I(t) + T_{iG}G(t) + T_{iGN}N(t)G(t), I(t_0) = I_b \quad (8)$$

Table 1 Definition of the symbols in (7) and (8).

Symbol	Units	Definition
t	min	Time
$G(t)$	mmol	Amount of ingested glucose in the duodenum
$I(t)$	pM	Plasma insulin concentration
$N(t)$	pM	Plasma GLP-1 concentration
$D(t)$	mmol	Amount of ingested glucose appearing in the duodenum
K_{xg}	min ⁻¹	The insulin-independent rate constant of tissue glucose uptake
K_{xgl}	min ⁻¹ /pM	The insulin-dependent rate constant of tissue glucose uptake
K_{gd}	min ⁻¹	The rate constant of glucose absorbed from the duodenum into the blood
K_{xi}	min ⁻¹	The disappearance rate constant for insulin
V_g	L	The distribution volume for glucose
T_{gl}	pM/min	The increase in plasma glucose concentration due to hepatic glucose release
G_b	mM	Glycemia at t_0
I_b	pM	Insulinemia at t_0
T_{iG}	pM/min/mM	The rate of pancreatic release of insulin due to glucose
T_{iGN}	pM/min/pM/mM	The rate of pancreatic release of insulin due to GLP-1

Hierarchical nonlinear models are typically applied to biostatistical problems. These models arise frequently in situations where several measurements are made on a number of subjects. Repeated measurements on a subject may be taken over time, at different analyte concentrations. The existence of repeated measurements requires particular care in characterizing the random variation in the data. In particular, it is important to recognize explicitly two levels of variability:

random variation among measurements within a given subject (intra-individual variation) and random variation among subjects (inter-individual variation).

Normally, specification of a distribution to characterize inter-individual variation is too difficult. There are many models to take into account such variation. In the present work, we used a Bayesian model specification to represent the inter-individual variation. A Bayesian nonlinear model involves 3 stages, according to Davidian and Giltinan [10], as in the following.

Stage I Intra-individual variation

In this stage, we specify the mean response and variance-covariance structure for a given subject.

$$y_{ij} = f_{xy}(\beta_k, t_{ij}) + e_{ij}, E(e_k | \beta_k) = 0, Cov(e_k | \beta_k) = R_k(\beta_k, \xi) \quad (9)$$

$$\text{where } R_k(\beta_k, \xi) = \begin{pmatrix} \sigma_G^2 f_G^2(\beta_k, t_{ij}) & 0 \\ 0 & \sigma_I^2 f_I^2(\beta_k, t_{ij}) \end{pmatrix} \quad (10)$$

$\xi = (\sigma_G^2, \sigma_I^2)$ is the variance-covariance vector parameter, and f_G and f_I are the mean responses for the glucose and insulin, respectively.

Stage II Inter-individual variation

The second stage involves a model for variation in the regression parameters θ_k . This variation can be due to systematic dependence on subject characteristics, such as gender, age or simply to biological variability among different individuals. In this work, we consider the simplest case of linear model:

$$\theta_k = \theta + b_k, b_k \sim N(0, D) \quad (11)$$

where $\theta_k = \log(\beta_k) = \log(K_{gd}, K_{xg}, K_{xgl}, K_{xi}, V_g)$, D denotes the joint covariance matrix for all random effects; and $\hat{\beta}_k$ is the individual estimate for Subject k .

Stage III Hyperprior distribution

The model specification is completed by an assumption of a distribution for all parameters in Stages 1 and 2: β, ξ and D :

$$\theta_k \sim N(\theta^*, \Sigma^*), D^{-1} \sim Wi(\rho, [\rho D^*]^{-1}), (\sigma^2)^{-1} \sim Gam\left(\frac{\nu_0}{2}, \frac{\tau_0 \nu_0}{2}\right)$$

where Wi and Gam represent Wishart and Gamma distributions, respectively.

C. MCMC Implementation

By following the studies of Davidian and Giltinan [10], Gelfand *et al.* [11] and Wakefield *et al.* [12], it can be shown from Stages 1, 2 and 3 that the full conditional distribution of the parameters-given the remaining parameters and the data, and for the parameters θ, D^{-1} and σ^2 , may be written explicitly as

$$\pi(\theta | y, \theta_1, \dots, \theta_m, D, \sigma_G^2, \sigma_I^2) = N(V(mD^{-1}\bar{\theta}) + \Sigma^{*-1}\theta, V) \quad (12)$$

$$\pi(D^{-1} | y, \theta, \theta_1, \dots, \theta_m, \sigma_G^2, \sigma_I^2) = Wi\left([\sum_{k=1}^m (\theta_k - \theta)(\theta_k - \theta)^T + \rho D^*]^{-1}, m + \rho\right) \quad (13)$$

$$\pi(\sigma_G^2 | y, \theta, \theta_1, \dots, \theta_m, D) = Gam\left(\frac{1}{2}(\nu_{0G} + N),\right)$$

$$\frac{1}{2}[\sum_{k=1}^m (y_k - f_G(\theta_k))^T (y_k - f_G(\theta_k)) + \nu_{0G} \tau_{0G}] \quad (14)$$

$$\pi(\sigma_I^2 | y, \theta, \theta_1, \dots, \theta_m, D) = Gam\left(\frac{1}{2}(\nu_{0I} + N),\right)$$

$$\frac{1}{2}[\sum_{k=1}^m (y_k - f_I(\theta_k))^T (y_k - f_I(\theta_k)) + \nu_{0I} \tau_{0I}] \quad (15)$$

However, the full conditional distribution of each θ_k , given the remaining parameters and the data, cannot be calculated explicitly but can be written up as a density function that is proportional to

$$\begin{aligned} \pi(\theta_k | y, \theta, \theta_j, j \neq i, \sigma_G^2, \sigma_I^2, D) &\propto \frac{1}{|R_k(\theta_k, \xi)|^{1/2}} \\ &\times \exp\left\{-\frac{1}{2}(y_k - f_k\{\theta_k\})^T R_k^{-1}(\theta_k, \xi)(y_k - f_k\{\theta_k\})\right\} \\ &\times \exp\left\{-\frac{1}{2}(\theta_k - \theta)^T D^{-1}(\theta_k - \theta)\right\} \end{aligned}$$

MCMC method is an algorithm for drawing samples $\{x_t, t = 1, 2, \dots\}$ throughout the Markov chain, which has the posterior distribution $\pi(\cdot)$ as its stationary distribution $\phi(\cdot)$. In the next stage, x_{t+1} is sampled from a distribution $P(x_{t+1} / x_t)$ depending only on the current stage of the chain- x_t . Since the Markov chain is an iteration method, we have to start at the stage x_0 that makes the initial stage of its chain gradually forgotten; the chain will eventually converge to a unique $\phi(\cdot)$ which depends neither on t nor x_0 . Thus, as t increases, the sample points $\{x_t\}$ will look increasingly like dependent samples from $\phi(\cdot)$. Consequently, after a sufficiently large number of m iterations, the points $\{x_t, t = m + 1, \dots, n\}$ will be approximately dependent samples from $\phi(\cdot)$.

There are many ways to obtain a Markov chain. In this work, we use the Gibbs sampling presented by Geman and Geman [13], to update θ, D^{-1} and σ^2 , while we update $\theta_k, k = 1, 2, \dots, 30$ by using the Metropolis–Hastings algorithm [14, 15], because the full conditional distribution of each θ_k , inside the Gibbs sampling, given the remaining parameters and the data, cannot be calculated explicitly.

The proceeding for MCMC method by using the Metropolis–Hastings algorithm inside the Gibbs sampling to draw the samples of the parameters from Bayesian posterior distribution is given as follows.

(1) Start with the initial values

$$\psi^{(0)} = (\sigma^{2(0)}, \theta^{(0)}, D^{-1(0)}, \gamma^{(0)})^T$$

where $\gamma = \{\theta_k, k = 1, 2, \dots, 30\}$ and choose $\theta_k^{(0)} = \theta^{(0)}$.

(2) Obtain a new value

$$\psi^{(i)} = (\sigma^{2(i)}, \theta^{(i)}, D^{-1(i)}, \gamma^{(i)})^T$$

from $\psi^{(i-1)}$ throughout the proposal distribution:

$$\begin{aligned} \sigma^{2(i)} &\sim \pi(\sigma^2 / y, \theta^{(i-1)}, D^{-1(i-1)}, \phi^{(j-1)}) \\ \theta^{(i)} &\sim \pi(\theta / y, \sigma^{2(i)}, D^{-1(i-1)}, \phi^{(j-1)}) \\ D^{-1(i)} &\sim \pi(D^{-1} / y, \sigma^{2(i)}, \theta^{(i)}, \phi^{(j-1)}) \end{aligned}$$

(3) For $\theta_k^{(i)}$, move a chain to a new value φ , which is generated from the proposal $q(\varphi / \theta_k^{(i-1)})$, from $\theta_k^{(i-1)}$. Evaluate

$$\alpha(\varphi / \theta_k^{(i-1)}) = \min \left(1, \frac{\pi(\varphi / y, \sigma^{2(i)}, \theta^{(i)}, D^{-1}, \phi_{\{k\}}^{(i-1)})}{\pi(\theta_k^{(i-1)} / y, \sigma^{2(i)}, \theta^{(i)}, D^{-1}, \phi_{\{k\}}^{(i-1)})} \right)$$

(4) Sample a uniform (0,1) random variable U . If $U \leq \alpha(\varphi / \theta_k^{(i-1)})$, then set $\theta_k^{(i)} = \varphi$, otherwise set $\theta_k^{(i)} = \theta_k^{(i-1)}$ and the chain does not move.

(5) Increase i , and return to (2) until convergence is reached.

D. GLS Procedure

We applied GLS, which is a two-stage method, by following the studies of Panunzi et al. [16]. We used the first run of MCMC to be an initial value for this method. The proceeding is given as follows.

Stage I

(1) In K separate estimation procedures (where K is the total number of subjects), obtain preliminary estimates $\hat{\beta}_k^{(p)}$ for each subject $k, k = 1, 2, \dots, K$, by using Ordinary Least Squares (OLS) estimator.

(2) Calculate residuals from (1) and estimate $\xi = (\sigma_G^2, \sigma_I^2)$ minimizing the following function:

$$PL = \sum_{k=1}^{30} (\log |R_k(\beta_k^{(p)}, \xi)| + [y_k - f_k(\beta_k^{(p)})]^T R_k^{-1}(\beta_k^{(p)}, \xi) [y_k - f_k(\beta_k^{(p)})])$$

(3) Construct estimated weight matrices which depend on the estimated parameters $\hat{\xi}$ and $\beta_k^{(p)}: \hat{R}_k(\beta_k^{(p)}, \hat{\xi})$.

(4) Use the estimated weight matrices from (3), re-estimate the β_k for each subject $k, k = 1, 2, \dots, 30$ by minimizing

$$[y_k - f_k(\beta_k)]^T R^{-1}(\beta_k^{(p)}, \xi) [y_k - f_k(\beta_k)]$$

The resulting estimates can be treated as preliminary estimates and it is possible to return to (2). The algorithm should be iterated at least once and for each Subject k . β_{iGLS} denotes the final estimates.

Stage II

We obtain β_{iGLS} from Stage I, then the population estimators of the vector β and the variance-covariance matrix D are obtained by

$$\hat{\beta} = \frac{1}{k} \sum_{i=1}^{30} \beta_{iGLS} \quad \text{and} \quad \hat{D} = \frac{1}{(m-1)} \sum_{i=1}^{30} (\hat{\beta}_{iGLS} - \hat{\beta})^T (\hat{\beta}_{iGLS} - \hat{\beta}).$$

III. RESULTS

The results of MCMC application are obtained in about ten days. The entire run involves 20,000 iterations and the first 5,000 iterations are considered as burn-in period, while the GLS application converges in 21 iterations. On the principle of choosing the initial values for MCMC, Gelfand [17] concludes that if MCMC samplers run long enough to forget its initial states, the results are not much difference.

Here, we performed three runs with initial values shown in Table 2. In performing MCMC and GLS estimations, the initial values for the subject parameters and population parameters θ^0 and θ_k^0 were set equal to the logarithm values

$$\theta^0 = \theta_k^0 = \log[K_{gd}, K_{xg}, K_{xgl}, K_{xi}, V_g].$$

Table 3 shows the point estimates (PM) for the three runs based on MCMC, We can see that, the results are close to the true values (TV) for every parameters. Moreover, in the first run, the PM for each parameter has a smaller bias. Figures 2, 3, 4, 5 and 6 show the trace of the sample values of the parameters $K_{gd}, K_{xg}, K_{xgl}, K_{xi}$ and V_g , respectively for three runs. All of them are seen to quickly settle down and stabilize.

As for the performance of GLS shown in Table 4, while the PM from the first run is closer to TV but in the second and the third runs, they are not close to the corresponding TV for every parameter, for example, for the parameter K_{xg} in the second run. So, we use the first run in Table 3 and Table 4 to compare the performances of MCMC and GLS. The initial values for the subject parameters θ_k^0 and population parameters θ^0 were set to

$$\theta^0 = \theta_k^0 = \log[0.05, 0.05, 0.00025, 0.025, 32.5].$$

Table 5 and Table 6 summarize the results on estimation of population parameters based on MCMC and GLS, respectively. In Table 7, we present the estimates of subject-specific individual parameters. For comparison, the true parameter values and estimation bias are also presented for each parameter. Figure 7, Figure 8 and Figure 9 show the curves of estimated values for Subject 1, Subject 18 and Subject 29, respectively. Moreover, the estimated subject parameters, the standard deviation (SD) and coefficient of variation (CV), based on MCMC method and GLS method, are also shown in Figure 10 and Figure 11.

Table 2 The initial values for parameters in three runs of the MCMC and GLS sampler.

Parameters	Run1	Run2	Run3
K_{gd}	0.05	0.1	0.004
K_{xg}	0.05	0.1	0.005
K_{xgl}	0.0025	0.0005	0.00005
K_{xi}	0.025	0.05	0.003
V_g	32.5	60	10

Table 3 The true values (TV) and point estimates (PM) of population parameters in comparison between three runs based on MCMC.

Parameters	TV	PM Run1	PM Run2	PM Run3
K_{gd}	0.04	0.04765	0.0498	0.0485
K_{xg}	0.001	0.00125	0.0048	0.0032
K_{xgl}	0.0001	0.000094	0.000083	0.000093
K_{xi}	0.03	0.0308	0.0274	0.027
V_g	14	16.23	16.63	16.43

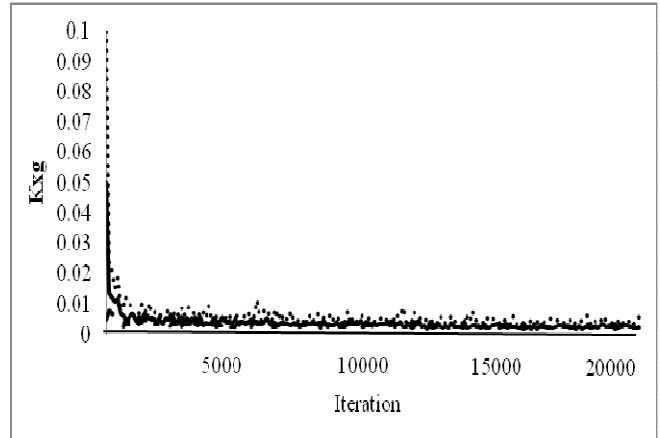


Fig. 3 Sampled values for K_{xg} from three runs of the MCMC method applied to the model: run1, solid line; run 2, dotted line; run3 broken line.

Table 4 The true values (TV) and point estimates (PM) of population parameters in comparison between three runs based on GLS.

Parameters	TV	PM Run1	PM Run2	PM Run3
K_{gd}	0.04	0.05463	0.0529	0.0532
K_{xg}	0.001	0.00232	0.0361	0.0215
K_{xgl}	0.0001	0.000109	0.000093	0.000108
K_{xi}	0.03	0.0312	0.0259	0.0273
V_g	14	19.29	16.7729	16.5774

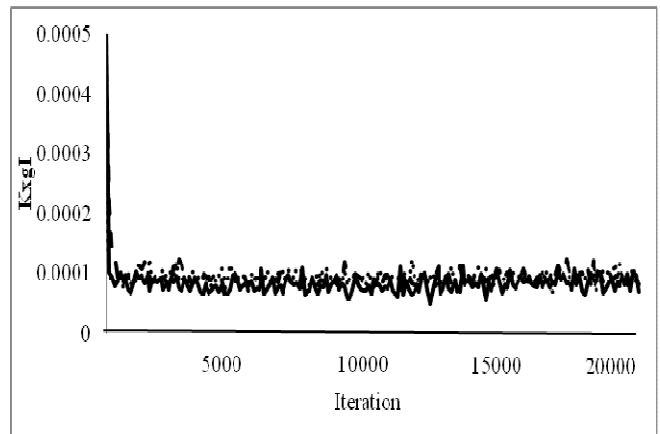


Fig.4 Sampled values for K_{xgl} from three runs of the MCMC method applied to the model: run1, solid line; run 2, dotted line; run3 broken line.

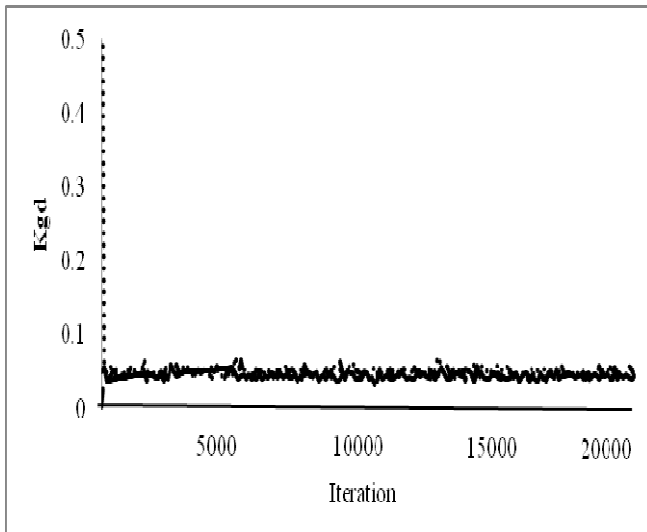


Fig. 2 Sampled values for K_{gd} from three runs of the MCMC method applied to the model: run1, solid line; run 2, dotted line; run 3 broken line.

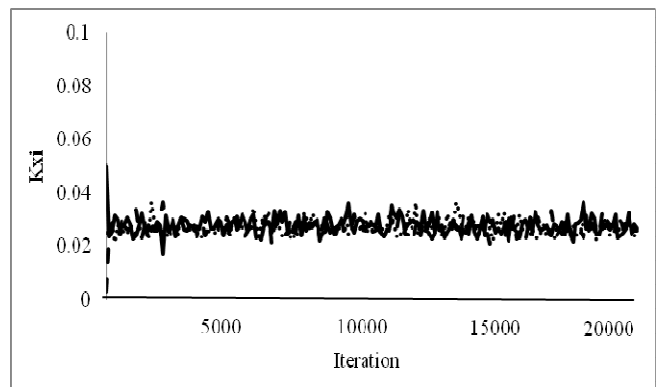


Fig.5 Sampled values for K_{xi} from three runs of the MCMC method applied to the model: run1, solid line; run 2, dotted line; run3 broken line.

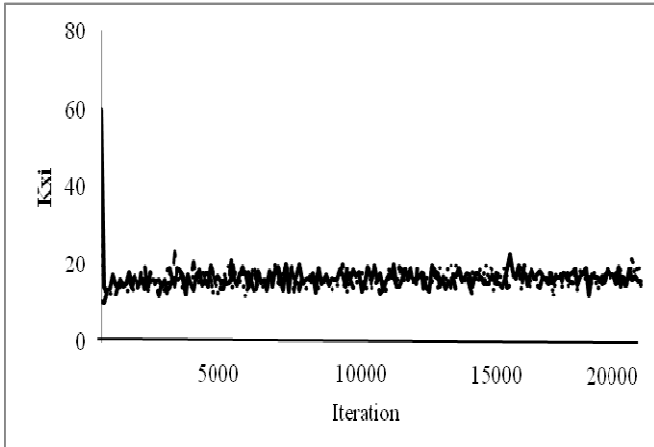


Fig.6 Sampled values for V_g from three runs of the MCMC method applied to the: run1, solid line; run 2, dotted line; run3 broken line.

Table 5 The true values (TV), posterior means (PM), standard deviation (SD) and 95% credible intervals (CI) of population parameters based on MCMC.

Parameters	TV	PM	SD	95% CI
K_{gd}	0.04	0.04765	0.0236	(0.0392,0.0561)
K_{xg}	0.001	0.00125	0.00039	(0.00112,0.0014)
K_{xgl}	0.0001	0.000094	0.00007	(0.000069,0.000119)
K_{xi}	0.03	0.0308	0.0146	(0.0256,0.0361)
V_g	14	16.23	13.07	(11.55,20.91)

Table 6 The true values (TV), point estimates (PM), standard deviation (SD) and 95% credible intervals (CI) of population parameters based on GLS.

Parameters	TV	PM	SD	95% CI
K_{gd}	0.04	0.05463	0.024	(0.0460,0.0632)
K_{xg}	0.001	0.00232	0.0012	(0.0018,0.0027)
K_{xgl}	0.0001	0.000109	0.00008	(0.000082,0.00013)
K_{xi}	0.03	0.0312	0.0159	(0.0256,0.0370)
V_g	14	19.29	14.62	(13.13,21.45)

Table 7 The true values (TV), point estimates (PM) and bias of population parameters in comparison between MCMC and GLS.

Parameters	TV	MCMC	Bias	GLS	Bias
K_{gd}	0.04	0.04765	-0.00765	0.05463	-0.01463
K_{xg}	0.001	0.00125	-0.00025	0.00232	-0.00132
K_{xgl}	0.0001	0.000094	0.000006	0.000109	-0.000009
K_{xi}	0.03	0.0308	-0.00084	0.0312	0.0013
V_g	14	16.23	-2.23	19.29	-5.29

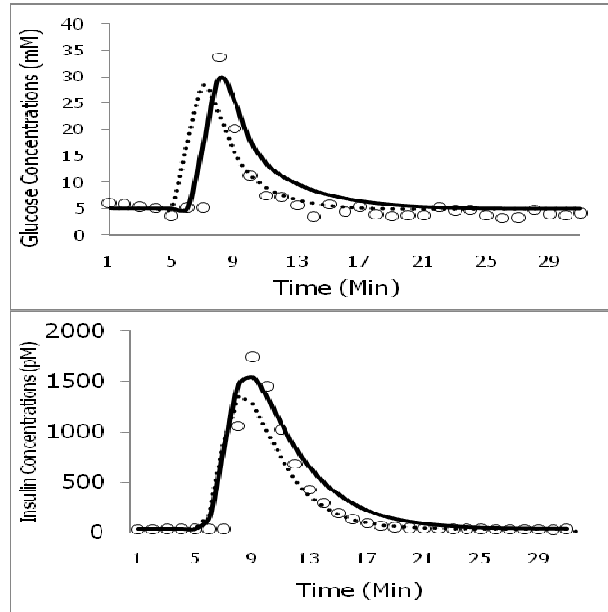


Fig. 7 Glucose and insulin concentrations versus time together with the predicted time-curves from the glucose/insulin model with GLP1-DPP4 interaction for Subject 1. The solid and dashed lines represent estimated subject curves based on MCMC and GLS, respectively. The generated values for Subject 1 are indicated by the open circles.

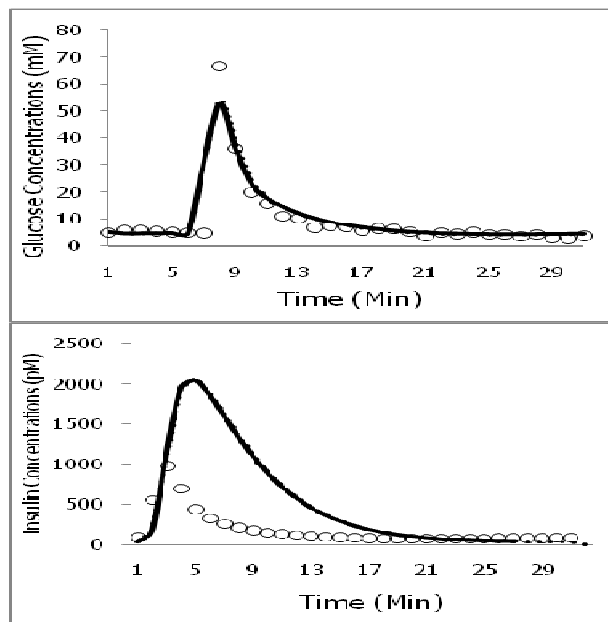


Fig. 8 Glucose and insulin concentrations versus time together with the predicted time-curves from the glucose/insulin model with GLP1-DPP4 interaction for Subject 18. The solid and dashed lines represent estimated subject curves based on MCMC and GLS, respectively. The generated values for Subject 18 are indicated by the open circles.

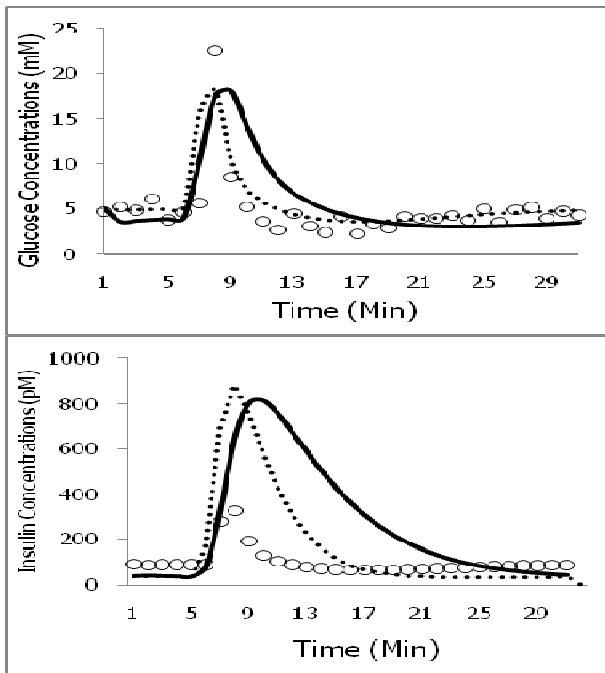


Fig. 9 Glucose and insulin concentrations versus time together with the predicted time-curves from the glucose/insulin model with GLP1-DPP4 interaction for Subject 29. The solid and dashed lines represent estimated subject curves based on MCMC and GLS, respectively. The generated values for Subject 29 are indicated by the open circles.

IV. CONCLUSION

The main aim of this study is to investigate the application of MCMC and GLS methods to estimate parameters in the glucose/insulin nonlinear differential model with GLP1-DPP4 interaction. From our comparison between MCMC and GLS results, we observe that, in the estimations of K_{gd} , K_{xg} , K_{xi} and V_g , the bias and standard deviation for any parameters with the use of MCMC are smaller than with GLS. Thus, this indicates that MCMC performs better than GLS in estimating every parameter in the glucose/insulin nonlinear differential model with GLP1-DPP4 interaction.

Based on the generated data, we suggest the use of MCMC instead of GLS for point estimation on the glucose/insulin nonlinear differential model with GLP1-DPP4 interaction because without any knowledge of the distribution of the data we can easily obtain more accurate posterior means through MCMC method than GLS method. Although, MCMC takes more time than GLS, MCMC would never give rise to such error as that arising from GLS.

This study is expected to add to the knowledge gained by previous works ([2]-[6], [8], [9], [18]-[21]) and benefit biostatistics researchers, especially those interested in Diabetes Mellitus, who may be able to select the appropriate method for parameter estimations in their models without any prior knowledge of the distribution of the data and when heterogeneity of variance is evident.

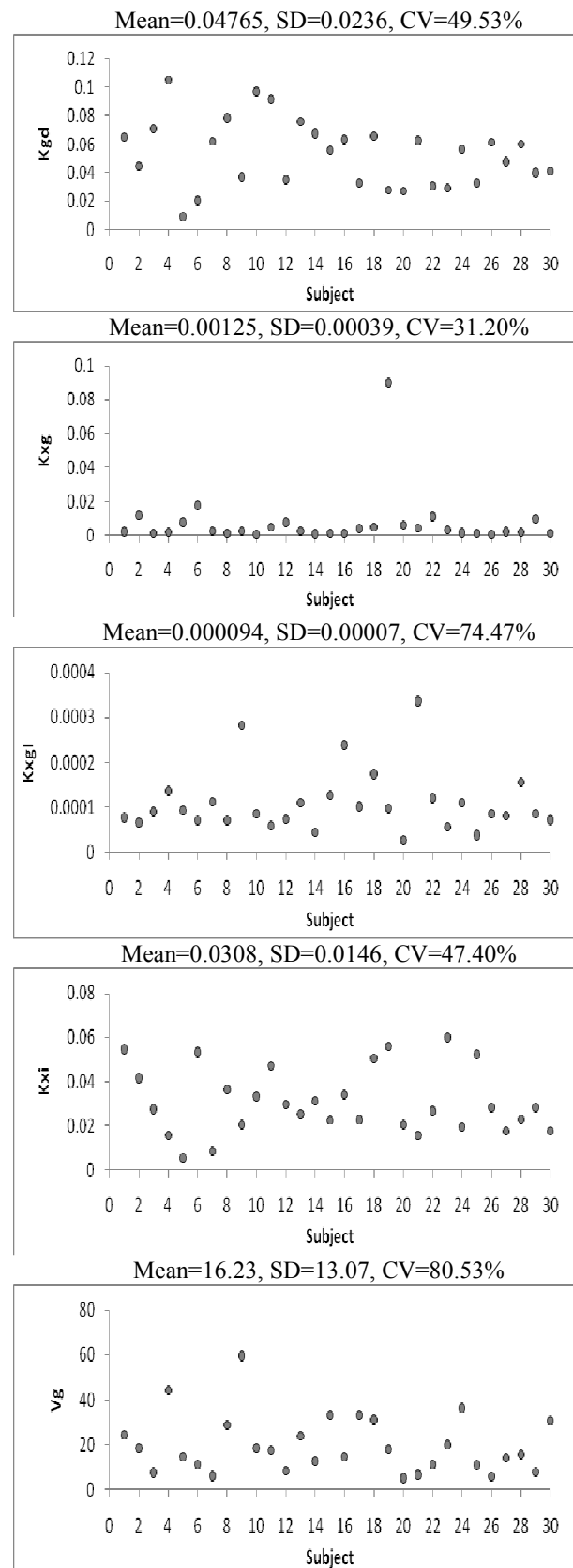


Fig. 10 The estimated subject parameters based on MCMC method. SD and CV=SD/PM stand for the standard deviation and coefficient of variation, respectively.

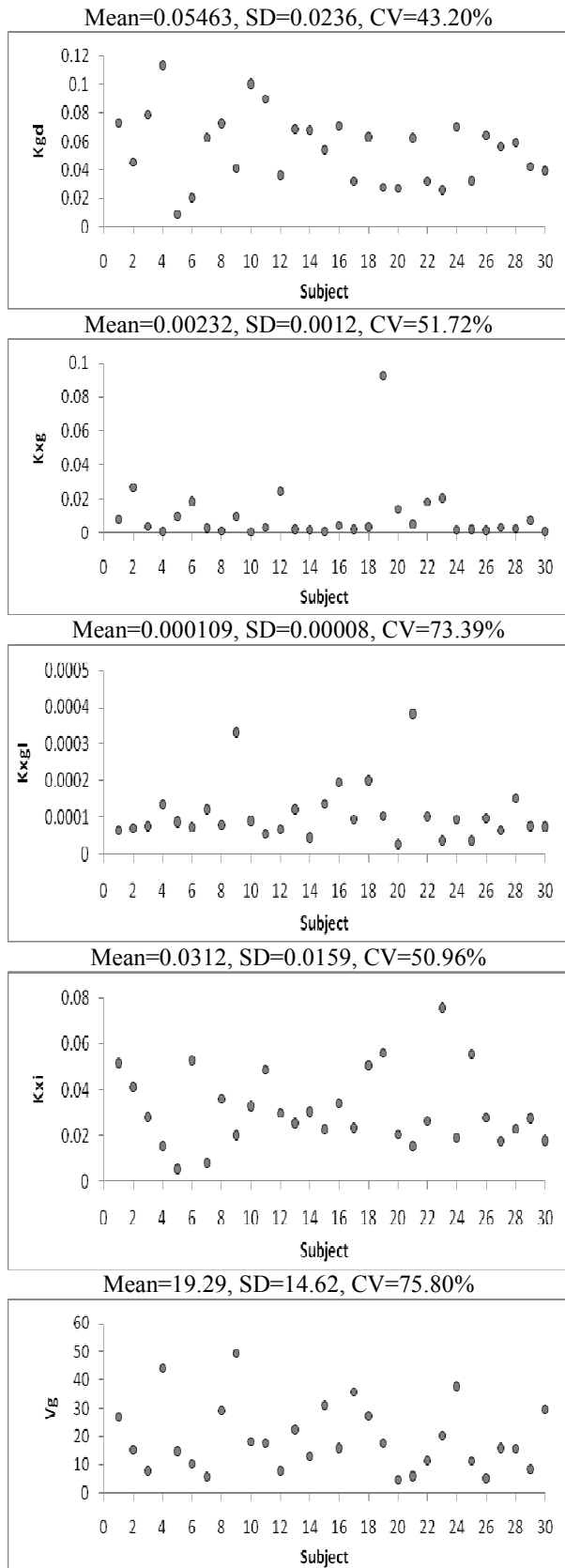


Fig. 11 The estimated subject parameters based on MCMC method. SD and CV=SD/PM stand for the standard deviation and coefficient of variation, respectively.

ACKNOWLEDGMENT

The first author has been supported by the Strategic Scholarships Fellowships Frontier Research Network, the Office of Commission on Higher Education and, together with the third and the fourth authors, BioMatLab CNR-IASI, Italy. The second author is supported by Mahidol University and the Centre of Excellence in Mathematics, CHE, Thailand.

REFERENCES

- [1] E. Rubin, H.M. Reisner, *Essentials of Robin's Pathology*, Ed Lippincott Williams & Wilkins, 2008.
- [2] R.N. Bergman, Y.Z. Ider, C.R. Bowden, C. Cobelli, Quantitative estimation of insulin sensitivity, *American Journal of Physiology*, Vol.236, 1979, pp. 667-677.
- [3] A. Boutayeb, A. Chetouani, A critical review of mathematical models and data used in diabetology, *Biomedical Engineering On Line*, Vol.5, 2006.
- [4] C.L. Chen, H.W. Tsai, S.S. Wong, Modeling the physiological glucose-insulin dynamic system on diabetics, *Journal of Theoretical Biology*, Vol.265, 2010, pp. 314-322.
- [5] A.D. Gaetano, O. Arino, Mathematical modeling of the intravenous glucose tolerance test, *Journal of Mathematical Biology*, Vol.40, 2000, pp. 136-168.
- [6] A. Makroglou, J. Li, Y. Kuang, Mathematical models and software tools for the glucose-insulin regulatory system and diabetes: an overview, *Applied Numerical Mathematics*, Vol.56, 2006, pp. 559-573.
- [7] M. Chuedoung, W. Sarika, Y. Lenbury, Dynamical analysis of a nonlinear model for glucose-insulin system incorporating delays and β -cells compartment, *Nonlinear Analysis*, Vol.71, 2009, pp. 1048-1058.
- [8] J. Schirra, B. Goke, *The physiological role of GLP-1 in human: Incretin, ileal brake or more, regulatory peptides*, 2005, pp. 109-115.
- [9] M. Bose, B. Oliván, J. Teixeira, F.X. Pi-Sunyer, B. Laferrère, *Do Incretins Play a Role in the Remission of Type 2 Diabetes after Gastric Bypass Surgery: What are the Evidence?*, *Obes Surg*, 2009, pp. 217-229.
- [10] M. Davidian, D.M. Giltinan, *Nonlinear models for Repeated Measurement Data*, Chapman & Hall, London, 1995.
- [11] A.L. Gelfand, S.E. Hills, A. Racine-Poon, A.F. M. Smith, Illustration of Bayesian inference in normal data models using Gibbs sampling, *Journal of the American Statistical Association*, Vol.85, 1990, pp. 972-985.
- [12] J.C. Wakefield, A.F.M. Smith, A. Racine-Poon, A.E. Gelfand, Bayesian analysis of linear and non-linear population models using the Gibbs sampler, *Applied Statistics*, Vol.43, 1994, pp.201-221.
- [13] S. Geman, D. Geman, Stochastic relaxation, Gibbs distributions, and the Bayesian restoration of images, *IEEE Trans Pattern Anal Mach Intell*, Vol. 66, 1984, pp. 721-741.
- [14] N. Metropolis, A.W. Rosenbluth, M.N. Rosenbluth, A.H. Teller, E. Teller, Equation of state calculation by fast computing machines, *The Journal of Chemical Physics*, Vol.21, 1953, pp.1087-1092.
- [15] W.K. Hastings, *Monte Carlo sampling methods using Markov chains and their applications*, *Biometrika*, Vol. 57, 1970, pp. 97-109.
- [16] S. Panunzi, P. Pasquale, D.G. Andrea, A discrete single delay model for the intra-venous glucose tolerance test, *Theoretical Biology and Medical Modelling*, Vol.26, 2007, pp.211-252.
- [17] A.E. Gelfand, *Markov Chain Monte Carlo in Practice*, Chapman & Hall, London, 1995.
- [18] E. Iancu, I. Iancu, M. Mota, Blood glucose data processing for automated diagnosis, *WSEAS Transaction on Biology and Biomedicine*, Vol. 5, 2008, pp. 75-84.
- [19] L. Kardar, A. Fallah, S. Gharibzadeh, F. Moztaaradeh, Application of fuzzy logic controller for intensive therapy in Type 1 Diabetic Mellitus patients by subcutaneous route, *WSEAS Transaction on Systems and Control*, Vol. 3, 2008, pp. 712-721.
- [20] P.O. Westermark, J.H. Kotaleski, A. Lansner, Derivation of a reversible Hill equations with modifiers affecting catalytic properties, *WSEAS Transaction on Biology and Medicine*, Vol. 1, 2004, pp. 91-98.

- [21] E. Iancu, I. Iancu, D. Istrate, M. Mota, Glucose level prediction using artificial neural networks, *Proceedings of the 9th WSEAS International Conference on Simulation, Modelling and Optimization*, 2009.